Phytomedicine 130 (2024) 155717

Contents lists available at ScienceDirect

Phytomedicine

journal homepage: www.elsevier.com/locate/phymed

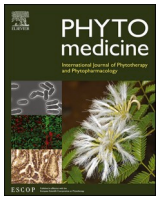

Original Article

Qiangxinyin formula protects against isoproterenol-induced cardiac hypertrophy

Zhong-Yan Zhou [a,b,c,1], Jie Ma [a,d,1,**], Wai-Rong Zhao [a,1], Wen-Ting Shi [a], Jing Zhang [a], Yan-Yan Hu [a], Mei-Yan Yue [a], Wen-Long Zhou [a], Hua Yan [e], Jing-Yi Tang [a,**], Yu Wang [b,c,*]

[a] *Longhua Hospital, Shanghai University of Traditional Chinese Medicine, Shanghai, China*
[b] *Department of Pharmacology and Pharmacy, The University of Hong Kong, Hong Kong Special Administrative Regions of China*
[c] *State Key Laboratory of Pharmaceutical Biotechnology, The University of Hong Kong, Hong Kong Special Administrative Regions of China*
[d] *School of Acupuncture-Moxibustion and Tuina, Shanghai University of Traditional Chinese Medicine, Shanghai, China*
[e] *Shuguang Hospital, Shanghai University of Traditional Chinese Medicine, Shanghai, China*

ARTICLE INFO

Keywords:
Heart failure
Cardiac fibrosis
Cardiac hypertrophy
Calcium overload
Traditional Chinese medicine
Zebrafish

ABSTRACT

Heart failure is a life-threatening cardiovascular disease and characterized by cardiac hypertrophy, inflammation and fibrosis. The traditional Chinese medicine formula Qiangxinyin (QXY) is effective for the treatment of heart failure while the underlying mechanism is not clear. This study aims to identify the active ingredients of QXY and explore its mechanisms protecting against cardiac hypertrophy. We found that QXY significantly protected against isoproterenol (ISO)-induced cardiac hypertrophy and dysfunction in zebrafish. Eight compounds, including benzoylmesaconine (BMA), atractylenolide I (ATL I), icariin (ICA), quercitrin (QUE), psoralen (PRN), kaempferol (KMP), ferulic acid (FA) and protocatechuic acid (PCA) were identified from QXY. PRN, KMP and icaritin (ICT), an active pharmaceutical ingredient of ICA, prevented ISO-induced cardiac hypertrophy and dysfunction in zebrafish. In H9c2 cardiomyocyte treated with ISO, QXY significantly blocked the calcium influx, reduced intracellular lipid peroxidative product MDA, stimulated ATP production and increased mitochondrial membrane potential. QXY also inhibited ISO-induced cardiomyocyte hypertrophy and cytoskeleton reorganization. Mechanistically, QXY enhanced the phosphorylation of Smad family member 2 (SMAD2) and myosin phosphatase target subunit-1 (MYPT1), and suppressed the phosphorylation of myosin light chain (MLC). In conclusion, PRN, KMP and ICA are the main active ingredients of QXY that protect against ISO-induced cardiac hypertrophy and dysfunction largely via the blockage of calcium influx and inhibition of mitochondrial dysfunction as well as cytoskeleton reorganization.

Introduction

Cardiovascular disease is the leading cause of death in the ageing population (Sutton et al., 2023). Heart failure is one of the life-threatening cardiovascular diseases and affects more than 64 million people worldwide (Savarese et al., 2023). Although various medications, for example angiotensin converting enzyme (ACE) inhibitors, angiotensin receptor/neprilysin inhibitors (ARNIs), beta-blockers, mineralocorticoid receptor antagonists (MRAs) and sodium–glucose co-transporter 2 (SGLT2) inhibitors, are commercially available

Abbreviations: ATL I, atractylenolide I; BMA, benzoylmesaconine; *ctnt2*, cardiac troponin T 2; *ckmb*, creatine kinase MB; *cnp*, C-type natriuretic peptide; dpf, day post-fertilization; DEGs, differentially expressed genes; EF, ejection fraction; FA, ferulic acid; GFP, green fluorescence protein; hpf, hour post-fertilization; ICA, icariin; ICT, icaritin; ISO, isoproterenol; KMP, kaempferol; MS, mass spectrometry; MLC, myosin light chain; MYPT1, myosin phosphatase subunit 1; NIF, nifedipine; P-MLC, phosphor myosin light chain 2; P-MYPT1, phosphor myosin phosphatase subunit 1; PRO, propranolol; PCA, protocatechuic acid; PRN, psoralen; QXY, Qiangxinyin; QCT, quercetin; QUE, quercitrin; RhoA, Ras homolog gene family member A; SIM, selected iron monitoring; S_{VED}, ventricular end-diastolic area; V_{VED}, ventricular end-diastolic volume; S_{VES}, ventricular end-systolic area; V_{VES}, ventricular end-systolic volume; α-SMA, α-smooth muscle actin.

* Corresponding author at: Department of Pharmacology and Pharmacy/State Key Laboratory of Pharmaceutical Biotechnology, Level 2, Laboratory Block, LKS Faculty of Medicine Building, The University of Hong Kong, 21 Sassoon Road, Pokfulam, Hong Kong Special Administrative Regions of China.
** Corresponding authors.
E-mail addresses: ma_chieh@126.com (J. Ma), dr_tang@163.com (J.-Y. Tang), yuwanghk@hku.hk (Y. Wang).
[1] These authors contributed equally to this work.

https://doi.org/10.1016/j.phymed.2024.155717
Received 9 February 2024; Received in revised form 8 April 2024; Accepted 5 May 2024
Available online 9 May 2024

Table 1
The constituents and proposed control standards of QXY formula.

No.	Chinese name	Pharmacopeia name	Species with Latin names	Amount (g)	Control standard				
					Name	CAS No.	Compound CID	Molecular formula	Molecular weight
1	附子	ACONITI LATERALIS RADIX PRAEPARATA	Aconitum carmichaelii Debx.	9	Benzoylmesaconine	63238–67–5	24832659	$C_{31}H_{43}NO_{10}$	589.70
2	白術	ATRACTYLODIS MACROCEPHALAE RHIZOMA	Atractylodes macrocephala Koidz.	12	Atractylenolide I	73069–13–3	5321018	$C_{15}H_{18}O_2$	230.30
3	淫羊藿	EPIMEDII FOLIUM	Epimedium brevicornu Maxim.	15	Icariin	489–32–7	5318997	$C_{33}H_{40}O_{15}$	676.70
4	豬苓	POLYPORUS	Polyporus umbellatus (Pers.) Fries	12	Quercitrin	522–12–3	5280459	$C_{21}H_{20}O_{11}$	448.40
5	補骨脂	PSORALEAE FRUCTUS	Psoralea corylifolia L.	15	Psoralen	66–97–7	6199	$C_{11}H_6O_3$	186.16
6	白芍	PAEONIAE RADIX ALBA	Paeonia lactiflora Pall.	9	Kaempferol	520–18–3	5280863	$C_{15}H_{10}O_6$	286.24
7	川芎	CHUANXIONG RHIZOMA	Ligusticum chuanxiong Hort.	12	Ferulic acid	1135–24–6	445858	$C_{10}H_{10}O_4$	194.18
8	茯苓	PORIA	Poria cocos (Schw.) Wolf	12	Protocatechuic acid	99–50–3	72	$C_7H_6O_4$	154.12
9	鹿角	CERVI CORNU	Cervus elaphus Linnaeus, Cervus Nippon Temminck	9	–	–	–	–	–

(Bauersachs, 2021), their efficacy is limited by off-target side effects, such as hypotension or bradycardia (Rosano et al., 2021). Understanding the pathological process of heart failure will facilitate effective drug development.

Traditional Chinese medicine has been used for the treatment of cardiovascular disease for thousands of years (Jia et al., 2020; Wang et al., 2017). The Qiangxinyin (QXY, 強心飲) formula, which consists of nine Chinese Materia Medica (Table 1), is derivate from Zhen Wu Decoction (真武湯) recorded in the Zhang Zhongjing's (張仲景) doctoral experience manuscript titled "Shanghan Lun" (傷寒論) in ancient China Han dynasty. QXY effectively improves the clinical symptom and cardiac function in patients with chronic heart failure (Yan Shiyun, 2004). In a rodent model of heart failure induced by doxorubicin, QXY ameliorates cardiac function and inhibits cardiomyocyte apoptosis by suppressing oxidative stress (Hu Jinping, 2023; Yan Hua, 2011). However, the active ingredients and underlying mechanisms of QXY are not fully understood.

Cardiac hypertrophy, inflammation and fibrosis are the key fundamental and antecedent pathological features of heart failure (McLellan et al., 2020). Zebrafish, a transparent vertebrate model sharing high genetic similarity with human, provides an alternative approach for mimicking cardiac dysfunction and hypertrophy (Kossack et al., 2017). The transgenic zebrafish line Tg (*cmlc2*: GFP) with specific green fluorescence protein (GFP) expression in cardiomyocyte has been well-established for cardiac function evaluation under fluorescence microscopy (Cheng et al., 2022; Ling et al., 2022; Wang et al., 2016), especially for the discovery of the cardioprotective ingredients from complex system like traditional Chinese medicine.

In the present research, we aim to explore the chemical profile of QXY using ultra high performance liquid chromatography – mass spectrometry (UHPLC-MS) technology and employ the zebrafish model as well as rat cardiomyocyte H9c2 to identify the active constitutes and the action mechanisms of QXY.

Materials and methods

Chemicals and reagents

Dimethyl sulfoxide (DMSO), thiazolyl blue tetrazolium (MTT), MS-222, isoproterenol (ISO), nifedipine (NIF) and propranolol (PRO) were purchased from Sigma-Aldrich (St. Louis, MO, USA). Benzoylmesaconine (BMA), atractylenolide I (ATL I), icariin (ICA), quercitrin (QUE), psoralen (PRN), kaempferol (KMP), ferulic acid (FA), protocatechuic acid (PCA), icaritin (ICT) and quercetin (QCT) were bought from Chengdu MUST Bio-technology (Chengdu, China). Enhanced mitochondrial membrane potential assay kit with JC-1, lipid peroxidation (MDA) kit, Actin-Tracker Red-Rhodamine and ATP detection kit were purchased from Beyotime Biotechnology (Shanghai, China). TriPure isolation reagent, RNeasy Mini Kit, cDNA Synthesis System for RT-PCR kit and SYBGREEN PCR Master Mix were brought from Roche (Basel, Switzerland). Fura-2 and DAPI were purchased from Thermo Fisher Scientific (Waltham, MA, USA). GAPDH (Cat No.5174S), Phosphor-Smad2 (Ser465/467)/ Smad3 (Ser423/425) (Cat No.8828S), Smad2 (Cat No.5339S), Phosphor-myosin phosphatase target subunit-1 (T853) (P-MYPT1, Cat No.4563S), myosin phosphatase target subunit-1 (MYPT1, Cat No.2634S), RhoA (Cat No.2117S), RhoA/Rho-kinase 1 (ROCK1, Cat No.4035S), Phosphor-Myosin Light Chain 2 (S19) (P-MLC, Cat No.3671S), Myosin Light Chain 2 (MLC, Cat No.3672S), Vimentin (Cat No.5741S), α-Smooth Muscle Actin (α-SMA, Cat No.19245S) and Anti-rabbit IgG (HRP-linked Antibody, Cat No.7074) were bought from Cell Signaling Technology (Danvers, Massachusetts, USA).

Preparation of QXY extract

Qiangxinyin formula (QXY) consists of nine Chinese Materia Medica, and their Chinese names, Pharmacopeia names, species with Latin names and dosages were listed in Table 1 according to the 2020 edition of the Chinese Pharmacopeia (Committee, 2020). The QXY was extracted by water for two times. Firstly, a total of 105 g QXY was boiled in 1050 ml distill water with reflux extraction, which was refer to the ratio of quality (g): volume (ml) = 1 : 10. The supernatant water extract was collected by filtration with filter paper (Whatman, Grade 598, Particle retention size 8–10 μm). Secondly, the QXY was boiled in 840 ml distill water with reflux extraction, which was refer to the ratio of quality (g) : volume (ml) = 1 : 8. The supernatant water extract was also collected by filtration and combined with the first water extract. Then, the QXY water extract was concentrated in a vacuum rotary evaporator (XD-2000A, Shanghai Xian De Experimental Instrument, Shanghai, China) with the condition of 50 ℃, −0.1 Mpa and 120 rpm, and followed by nitrogen blowing in a blowing concentrator (NAI-DCY-24Y, Shanghai Na Ai Precision Instrument, Shanghai, China) under 50 ℃ and until the weight not loss. Finally, we got 14.468 g QXY extract with the yield of 13.7779 % and it was kept in −80℃ for further use. QXY extract was dissolved in DMSO to form a 100 mg/ml stock solution for the following experiments in both cell and zebrafish models.

Table 2
Specific primers of zebrafish genes used in real-time PCR.

Accession number	Gene name	Forward primer	Reverse primer
NM_152,893.1	*ctnt2*	5′-CAGTGACCATCAGAAAACGTC-3′	5′-TTTCAACAGTGGTCAGCTCC-3′
NM_001109940.1	*cnp*	5′-AGCCGGATCTAAGAAAGGCG-3′	5′-ATCCCGCTCATGGTCCCTAT-3′
XM_005157593.1	*ckmb*	5′-CGTGACTGGTCTGACGGTAG-3′	5′-TCCTCGTTCACCCACACAAG-3′
NM_213,094.2	*gapdh*	5′-GCTTGGCTCCTCTGGCTAAA-3′	5′-GTCTTCTGTGTGGCGGTGTA-3′

Qualitive and quantitative analysis of constituents in QXY extract by UHPLC-MS technology

The QXY extract was preciously weighted two samples 0.245 g (Sample 1) and 0.251 g (Sample 2), and they were dissolved in 5 ml methanol and followed by supersonic extraction (250 W, 40 kHz, RT) for 30 min respectively. Then the extractions were centrifuged at 1200 rpm for 10 min and the supernatants were filtered by a 0.22 μm filter membrane for further analysis. The control standards listed in Table 1 were also prepared according to the above procedure and got the stock solution (10 μg/ml), and the mix standards sample was finally prepared with the concentration equal to 1 μg/ml of each compound. All the samples were measured and analyszed by the Thermo Scientific Q Exactive system which occupied with a Dionex Ultimate 3000 UHPLC system, an ACQUITY UPLC HSS T3 chromatographic column (2.1 mm×100 mm, 1.8 μm, Waters, USA) and a quadrupole/electrostatic field orbitrap high resolution mass spectrometry (MS) detector according to our previous study (Zhou et al., 2019a). The chromatographic analysis condition followed by gradient elution using aqueous 0.1 % formic acid (I) and acetonitrile (II) (0∼12 min, 5 %–95 % II; 12∼14 min, 95 % II; 14.01 min, 5 % II; 14.01∼16 min, 5 % II) accompanied with the flow velocity of 0.3 ml/min, column temperature of 45℃ and injection volume of 3 μl. The parameters of MS detector were as follows: Iron source, HESI; Positive and negative detection model, with spray voltage of +3.5 KV and −2.8 KV respectively; Auxiliary gas volume flow rate, 13 l/min; Sheath gas flow, 80 l/min; Capillary temperature, 320℃; Auxiliary gas heating temperature, 350℃; Collision energy, 30 eV; Detection model, full MS with resolution of 70,000, mass scan range of *m/z* 80∼1200. The external label one point method was used for the quantification of constitutes in QXY extract with average in sample 1 and 2.

Zebrafish maintenance and embryos collection

Wild type zebrafish and cardiomyocyte specifically expressed green fluorescence protein (GFP) zebrafish line Tg (*cmlc2*: GFP) were kindly provided by Prof. Simon Lee from The University of Macau and maintained as described in the fourth edition of The Zebrafish Book: A guide for the laboratory use of zebrafish Danio (Brachydanio) rerio by Monte Westerfield, Institute of Neuroscience, University of Oregon according to our previous studies (Zhao et al., 2021; Zhou et al., 2020a). Briefly, zebrafish was fed twice a day with fresh brine shrimp under a 14-h/10-h light-dark cycle in a 28.5℃ water-cycling system with a standard condition (pH 7.0∼8.0, conductivity 500∼800 μS/cm). The zebrafish embryos were collected by 2 females mating with 1 male within 1 h. Embryos were raised in E3 medium (5 mM NaCl, 0.17 mM KCl, 0.33 mM $CaCl_2$, 0.33 mM $MgSO_4$) and cultured in a petri dish at 28.5 °C. The zebrafish embryos were anaesthetized by MS-222 or ice water before sacrifice. And all the experimental protocols were in accordance with the ethical guidelines of Care and Use of Laboratory Animals and approved by Longhua Hospital – Animal Ethics Committee of Shanghai University of Traditional Chinese Medicine.

Toxicity analysis of QXY extract and its constituents in zebrafish

One day post-fertilization (dpf) wild type zebrafish embryos were distributed in 12-well plastic culture plates with 10 embryos/well. The zebrafish embryos were treated with various concentrations of QXY extract (3, 10, 30, 100, 300 and 1000 μg/ml) or its constitutes (3, 10, 30, 100 and 300 μM) including BMA, ATL I, ICA, QUE, PRN, KMP, FA and PCA for 5 days, and the survival rate of each group was recorded every day. The non-toxic concentrations of these compounds were applied in the following studies.

Zebrafish cardiac hypertrophy and function evaluation

Twenty-four hour post-fertilization (hpf) Tg(*cmlc2*: GFP) zebrafish embryos were distributed in 12-well plastic culture plates with 10 embryos/well. The zebrafish embryos were treated with ISO (1 mM), with or without various concentrations of QXY extract (100, 200 and 600 μg/ml) or its constitutes including BMA (30, 100 and 300 μM), ATL I (1, 3 and 10 μM), ICA (10, 30 and 100 μM), QUE (30, 100 and 300 μM), PRN (1, 3 and 10 μM), KMP (30, 100 and 300 μM), FA (30, 100 and 300 μM), PCA (10, 30, 100 and 300 μM), ICT (10, 30 and 100 μM) and QCT (30, 100 and 300 μM), for 48 hrs. Then the systolic and diastolic morphology of ventricle were observed and recorded under an inverted fluorescence microscope (Ti-U, Nikon, Japan). The volume of ventricle was calculated using the formula for a prolate spheroid: $V = \frac{4}{3}\times\pi\times\frac{a}{2}\times(\frac{b}{2})^2$. The area of ventricle was calculated using the formula for an oval: $S = \pi\times\frac{a}{2}\times\frac{b}{2}$. In the formula, the longitudinal axis was represented by a while the lateral axis was represented by b. The heart rate, cardiac output, stroke volume, ejection fraction (EF), fractional shortening (FS), ventricular end-diastolic area (S_{VED}), ventricular end-systolic area (S_{VES}), S_{VED} - S_{VES} (ΔS), ventricular end-diastolic volume (V_{VED}) and ventricular end-systolic volume (V_{VES}) were calculated (Wang et al., 2016) by a NIS Elements BR analysis software (Nikon, Japan).

mRNA expression level detection by real-time PCR

Twenty-four hpf wild type zebrafish embryos treated with ISO (1 mM), with or without QXY extract (600 μg/ml), for 48 h. The mRNA expression of C-type natriuretic peptide (*cnp*), creatine kinase MB (*ckmb*) and cardiac troponin T 2 (*ctnt2*) were detected by real-time PCR according to our previous studies (Zhao et al., 2021; Zhou et al., 2023). Briefly, the total RNA was extracted by RNeasy Mini Kit (Roche) and its concentration was quantified by OD260nm using multiple functional microplate reader occupied with NanoQuant microplate (M200, Tecan). Then the mRNA was reverse-transcripted by cDNA Synthesis System for RT-PCR kit (Roche), and the mRNA expression level of interested gene was detected with SYBGREEN PCR Master Mix (Roche) based on a light cycle 96 real-time PCR system (Roche). The specific primers of interested genes were listed in Table 2, and *gapdh* was served as the internal control. Finally, the expression levels of these genes were measured by $2^{-\Delta\Delta Ct}$ relative quantification method and presented as folds of the control group.

Transcriptome analysis by RNA-seq

Twenty-four hpf wild type zebrafish embryos were distributed in 6-well plastic plate with 50 fishes in each well. Zebrafish embryos were treated with or without QXY extract (600 μg/ml) for 48 h with 3 replicates in each group, then the total RNA of each sample was extracted by trizol reagent and followed by RNA-seq according to our previous studies (Zhou et al., 2020a). Briefly, the RNA concentration was quantified by Qubit® 2.0 Flurometer (Life Technologies, CA, USA), and the

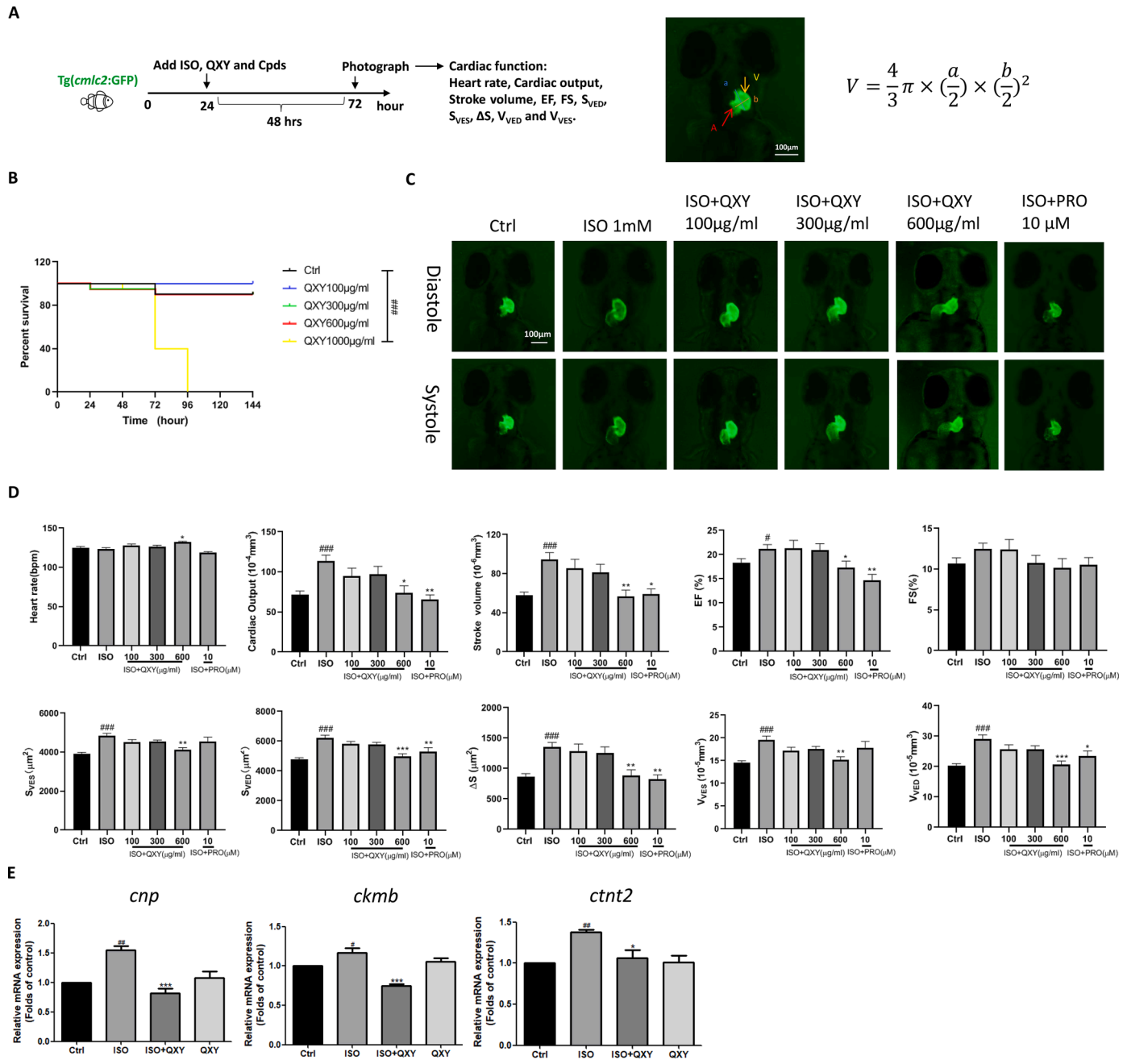

Fig. 1. The protective effect of QXY on the ISO-induced cardiac hypertrophy, dysfunction and injury in zebrafish. (A) Experimental flow and the demonstration of cardiac imaging and calculation of ventricular volume in transgenic zebrafish Tg (*cmlc2*: GFP) embryos. (B) The survival curve of 24 h post-fertilization (hpf) zebrafish embryos treated with various concentrations (100, 300, 600 and 1000 μg/ml) of QXY extract for 5 days. (C) The pictures demonstrated the end-diastolic and systolic images of ventricle in various treatment groups. (D) Twenty-four hpf zebrafish embryos were treated with ISO (1 mM), with or without various concentrations (100, 200 and 600 μg/ml) of QXY extract, for 48 h, then the cardiac morphology was observed by an inverted fluorescence microscope as well as the calculation of heart rate, cardiac output, stroke volume, ejection fraction (EF), fractional shortening (FS), ventricular end-diastolic area (S_{VED}), ventricular end-systolic area (S_{VES}), S_{VED} - S_{VES} (ΔS), ventricular end-diastolic volume (V_{VED}) and ventricular end-systolic volume (V_{VES}). Co-treatment of the beta-blocker propranolol (PRO, 10 μM) with ISO (1 mM) served as the positive control. (E) Twenty-four hpf zebrafish embryos were treated with ISO (1 mM), with or without QXY extract (600 μg/ml), for 48 h, then the mRNA expression levels of C-type natriuretic peptide (*cnp*), creatine kinase MB (*ckmb*) and cardiac troponin T 2 (*ctnt2*) were measured by real-time PCR, and the results were presented as folds of the control group. All the data were presented as mean ± SEM. $\#p < 0.05$ and $\#\#\#p < 0.001$ *vs* control (Ctrl) group; $*p < 0.05$, $**p < 0.01$ and $***p < 0.001$ *vs* ISO-treated group.

quality of the RNA was measured by the 2100 RNA Nano 6000 Assay Kit (Agilent Technologies, CA, USA). Construction of the sequencing library and RNA sequencing were performed by TIANGEN (Beijing, China) using the Illumina HiSeqTM4000 Platform. The differentially expressed genes (DEGs) were identified by DESeq2 with the criteria of false discovery rate (FDR) < 0.05 and fold change (FC) > 0.64. The DEGs were visualized by volcano plot and the Gene Ontology (GO) enrichment analysis was used for the classification of the DEGs in terms of the molecular function (MF), cellular component (CC) and biological process (BP).

Calcium (Ca^{2+}) imaging

The rat cardiomyocyte H9c2 was purchased from ATCC (CRL-1446).

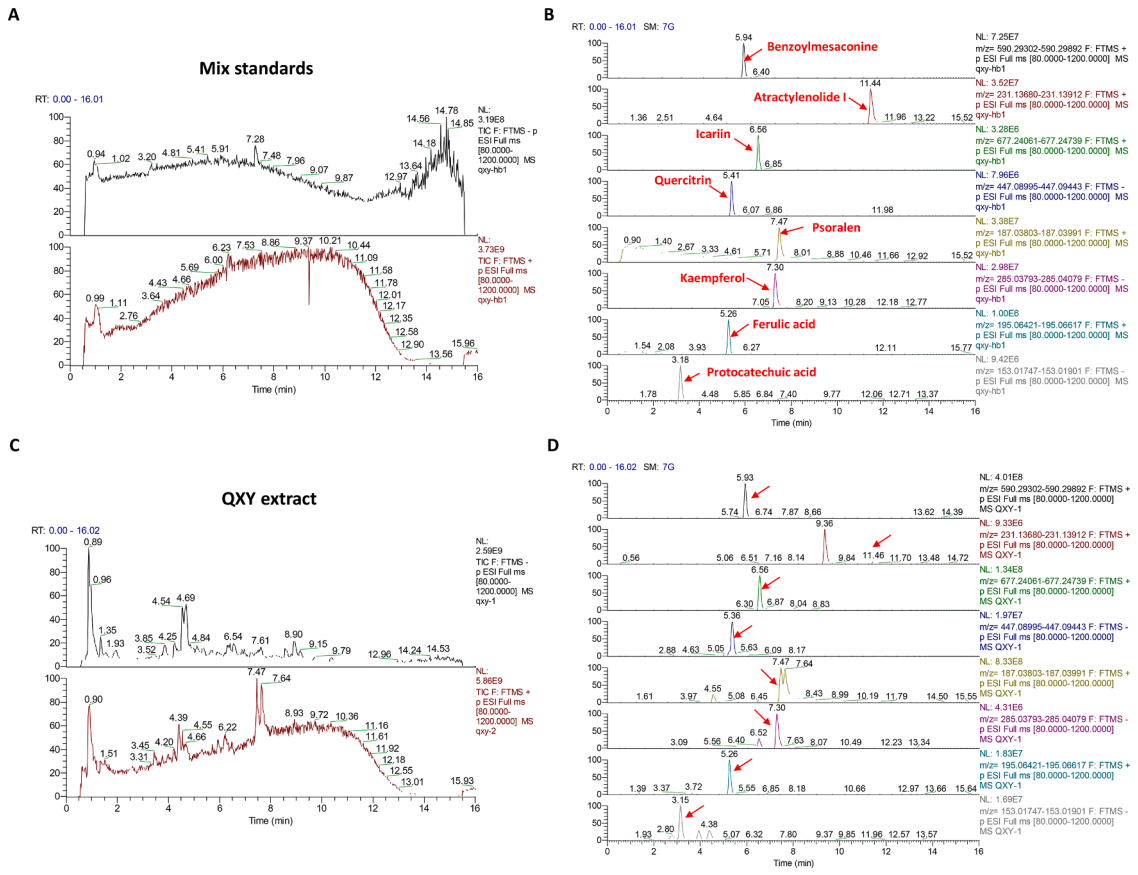

Fig. 2. The qualitative and quantitive analysis of the main contents of QXY extract by UHPLC-MS. (A-B) The total iron current in both positive and negative models and single iron monitor of mix standards including benzoylmesaconine, atractylenolide I, icariin, quercitrin, psoralen, kaempferol, ferulic acid and protocatechuic acid. (C-D) The total iron current in both positive and negative models and selected iron monitoring (SIM) of QXY extract. Red arrows indicated the standards or compounds in QXY extract. Retention times: Benzoylmesaconine, 5.93 min; Atractylenolide I, 11.46 min; Icariin, 6.56 min; Quercitrin, 5.36 min; Psoralen, 7.47 min; Kaempferol, 7.30 min; Ferulic acid, 5.26 min; Protocatechuic acid, 3.13 min.

Table 3
The content determination of components in QXY extract by UHPLC-MS.

No.	Compound name	Content in Sample 1 (μg/g)	Content in Sample 2 (μg/g)	Average Content (Mean ± *S.* D.)
1	Benzoylmesaconine (BMA)	119.86	129.02	124.44 ± 6.48
2	Atractylenolide I (ATL I)	0.38	0.47	0.42 ± 0.06
3	Icariin (ICA)	987.85	1086.05	1036.95 ± 69.44
4	Quercitrin (QUE)	77.58	78.70	78.14 ± 0.79
5	Psoralen (PRN)	988.65	979.96	984.30 ± 6.14
6	Kaempferol (KMP)	3.03	3.32	3.18 ± 0.21
7	Ferulic acid (FA)	400.53	431.27	415.90 ± 21.74
8	Protocatechuic acid (PCA)	39.31	40.41	39.86 ± 0.78

The cells were cultured in DMEM supplemental with 10 % FBS and 1 % PS in 37 ℃ incubator with 5 % CO_2 in atmosphere. The cells were seeded in 20 mm glass bottom cell culture dish (Biosharp) with the density of 1 × 10^5 cell/dish and cultured for 24 h, then followed by calcium probe loading, drug treatment and intracellular Ca^{2+} imaging. Firstly, the cells were staining with Ca^{2+} indicator Fura-2 (1 μM) for 20 min in Tyrode's solution (137 mM NaCl, 5.4 mM KCl, 1.0 mM $MgCl_2$, 10 mM HEPES, 10 mM Glucose and 1.8 mM $CaCl_2$), then wash with Tyrode's solution three times. Secondly, the cells were treated with QXY (20 μg/ml) or NIF (2 μM) which served as the positive control for 15 min according to our experimental design. Finally, the intracellular Ca^{2+} change was stimulated by ISO (1 μM) and real-time recorded by elimination of 340 nm/380 nm under fluorescence microscope (Nikon Ti-E, Japan) that occupied with Shutter light source and CMOS camera according to our previous study (Zhou et al., 2019b). The intracellular Ca^{2+} change was presented as the real-time fluorescence intensity (F1) to the fluorescence intensity before stimulation (F0).

Mitochondrial membrane potential and cytoskeleton staining

The H9c2 cells were seeded in 24-well cell culture plate with a density of 3 × 10^4 cell/well and cultured for 24 h. The cells were treated with ISO (100 μM), with or without various concentration of QXY (3 μg/ml and 5 μg/ml), for 24 h. For mitochondrial membrane potential staining, the cells were stained with JC-1 for 20 min at 37 ℃. The cells were photographed with the filters of GFP and Cy3 for green monomeric JC-1 and red aggregated JC-1 respectively using inverted fluorescence microscopy (Ti-U, Nikon, Japan). The mitochondrial membrane potential change was calculated by the fluorescence intensity ratio of Green/Red. For the cytoskeleton staining, the cells were fixed by 4 % PFA for 30 min at room temperature, then followed by staining with Actin-Tracker Red-Rhodamine for 30 min. The cells were counter stained with DAPI before image by inverted fluorescence microscopy (Ti-U, Nikon, Japan) using the filters of Cy3 and UV respectively. The intracellular cytoskeleton amount was calculated by the area of red cytoskeleton normalized with cell number.

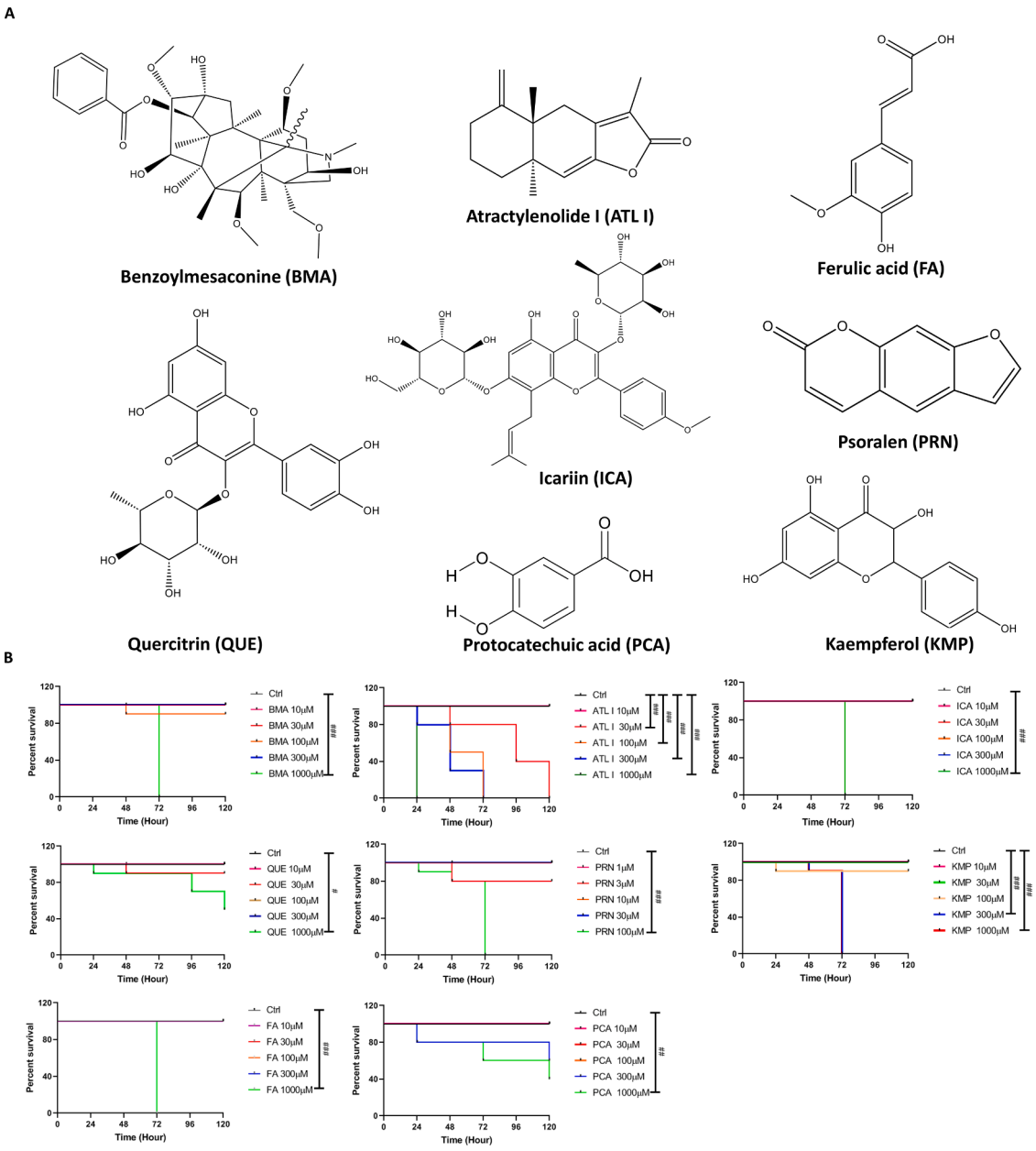

Fig. 3. The chemical structures of QXY ingredients and their toxicity profiles in zebrafish. (A) The chemical structures of QXY ingredients. (B) The survival curve of 24 hpf zebrafish embryos treated with indicated concentrations of benzoylmesaconine (BMA), atractylenolide I (ATL I), icariin (ICA), quercitrin (QUE), psoralen (PRN), kaempferol (KMP), ferulic acid (FA) and protocatechuic acid (PCA) for 5 days. $\#p < 0.05$, $\#\#p < 0.01$ and $\#\#\#p < 0.001$ *vs* control (Ctrl) group.

Intracellular lipid peroxidation (MDA) and ATP assays

The H9c2 cells were seeded in 6-well cell culture plate with a density of 1.6×10^5 cell/well and cultured for 24 h. The cells were treated with ISO (100 μM), with or without QXY (5 μg/ml), for 24 h. Then, the cells were collected and followed by intracellular MDA and ATP detection according to manufactures. The protein concentration was measured by BCA assay. The results were normalized by protein concentration and presented as folds of the control group.

Western blotting

The H9c2 cells were seeded in 6-well cell culture plate with a density of 1.6×10^5 cell/well and cultured for 24 h. The cells were treated with ISO (100 μM), with or without QXY (5 μg/ml), for 24 h. The western blotting procedure was following with our previous studies (Zhang et al., 2022; Zhou et al., 2023). Briefly, the cells were collected and lysis by RIPA buffer, and followed by protein concentration measurement using BCA kit. Twenty microgram protein of each sample was applied for denaturation and separation using SDS-PAGE gel electrophoresis. The proteins were transferred to PVDF membrane (0.45 μm), and the membrane was blocked in 5 % non-fat milk for 2 h at room temperature. Then the membrane was incubated with primary antibody (1:1000) overnight at 4°C and followed by the incubation with HRP-linked secondary antibody for 2 h at room temperature. Finally, the protein bands were visualized by the addition of ECL reagent and imaged by an imaging system (GE AM600, Fairfield, CT, USA). The integrated density of each protein band was analyzed by Image J software with normalization to internal control GAPDH.

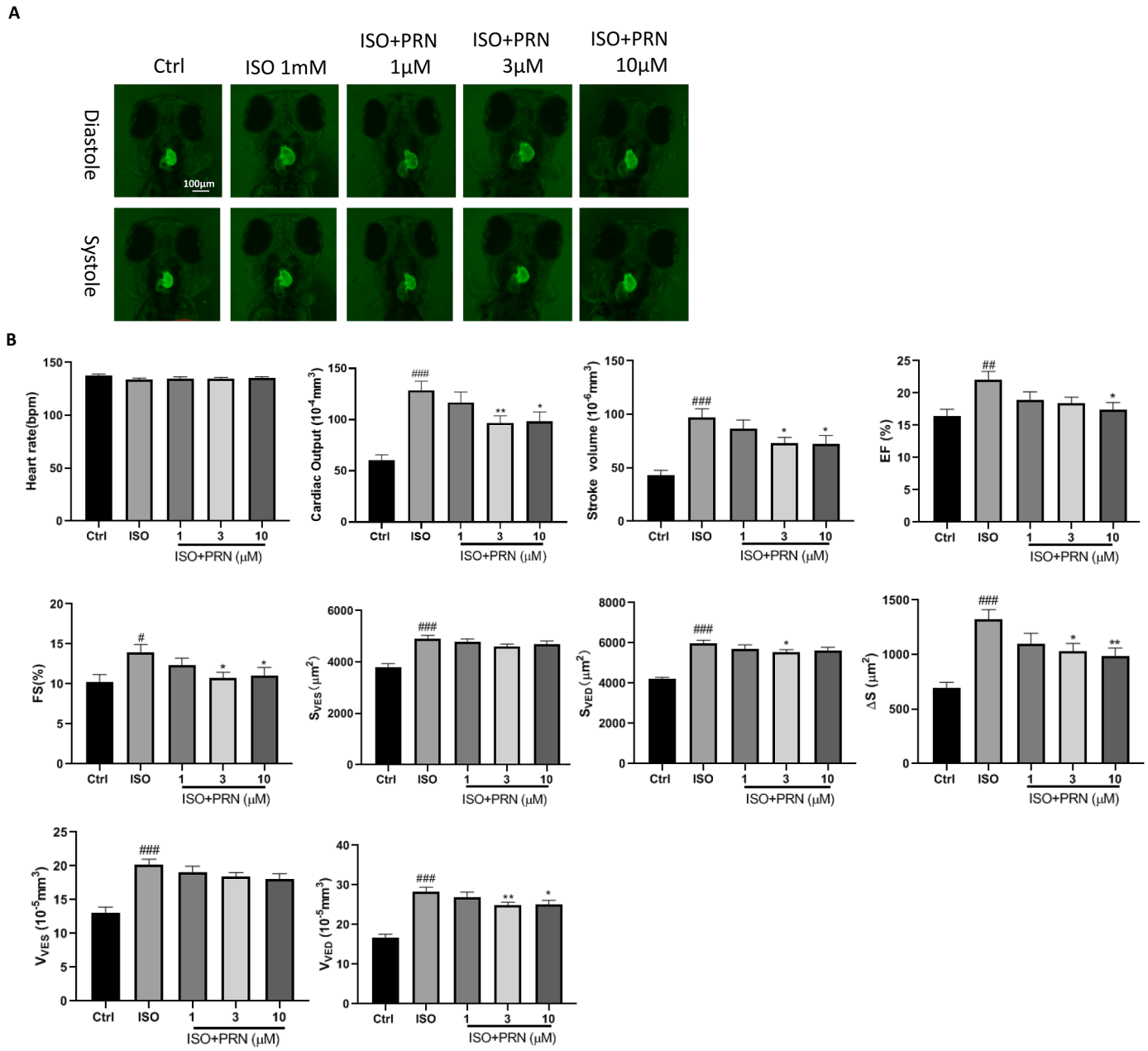

Fig. 4. The protective effect of psoralen (PRN) on ISO-induced cardiac hypertrophy and dysfunction in zebrafish. (A) The pictures demonstrated the end-diastolic and systolic image of ventricle in various treatment groups. (B) Twenty-four hpf zebrafish Tg(*cmlc2*: GFP) embryos were treated with ISO (1 mM), with or without various concentrations (1, 3 and 10 μM) of PRN, for 48 h, then the cardiac morphology was observed by an inverted fluorescence microscope as well as the calculation of heart rate, cardiac output, stroke volume, EF, FS, S_{VED}, S_{VES}, ΔS, V_{VED} and V_{VES}. All the data were presented as mean ± SEM. $\#p < 0.05$ and $\#\#\#p < 0.001$ *vs* control (Ctrl) group; $*p < 0.05$, $**p < 0.01$ and $***p < 0.001$ *vs* ISO-treated group. $n = 4–6$.

Statistical analysis

Each experiment has been repeated at least three times independently. Data were presented as mean ± SEM. All the data were analyzed and graphed by Prism GraphPad software (version 8.0). Student's *t*-test and One-way ANOVA were used to evaluate the significant difference between two groups, and $p < 0.05$ was considered significantly.

Results

QXY ameliorated ISO-induced cardiac hypertrophy, dysfunction and injury in zebrafish

Transgenic zebrafish Tg (*cmlc2*: GFP) embryos with heart-specific expression of GFP were employed to establish isoproterenol (ISO)-induced cardiac hypertrophy (Kossack et al., 2017). Heart rate, cardiac output, stroke volume, ejection fraction (EF), fractional shortening (FS), ventricular end-diastolic area (S_{VED}), ventricular end-systolic area (S_{VES}), S_{VED} - S_{VES} (ΔS), ventricular end-diastolic volume (V_{VED}) and ventricular end-systolic volume (V_{VES}) were selected as the key evaluation criteria of cardiac function (Fig. 1A). QXY within the concentration of 300 μg/ml did not significantly cause zebrafish death (Fig. 1B). ISO (1 mM) dramatically increased cardiac output, stroke volume, EF, S_{VED}, S_{VES}, ΔS, V_{VED} and V_{VES} than the control group although the heart rate and FS were not significantly change. Co-treatment with various concentrations of QXY extract (100, 200 and 600 μg/ml) significantly decreased the cardiac output, stroke volume, EF, S_{VED}, S_{VES}, ΔS, V_{VED} and V_{VES} in a concentration-dependent manner (Fig. 1C and D).

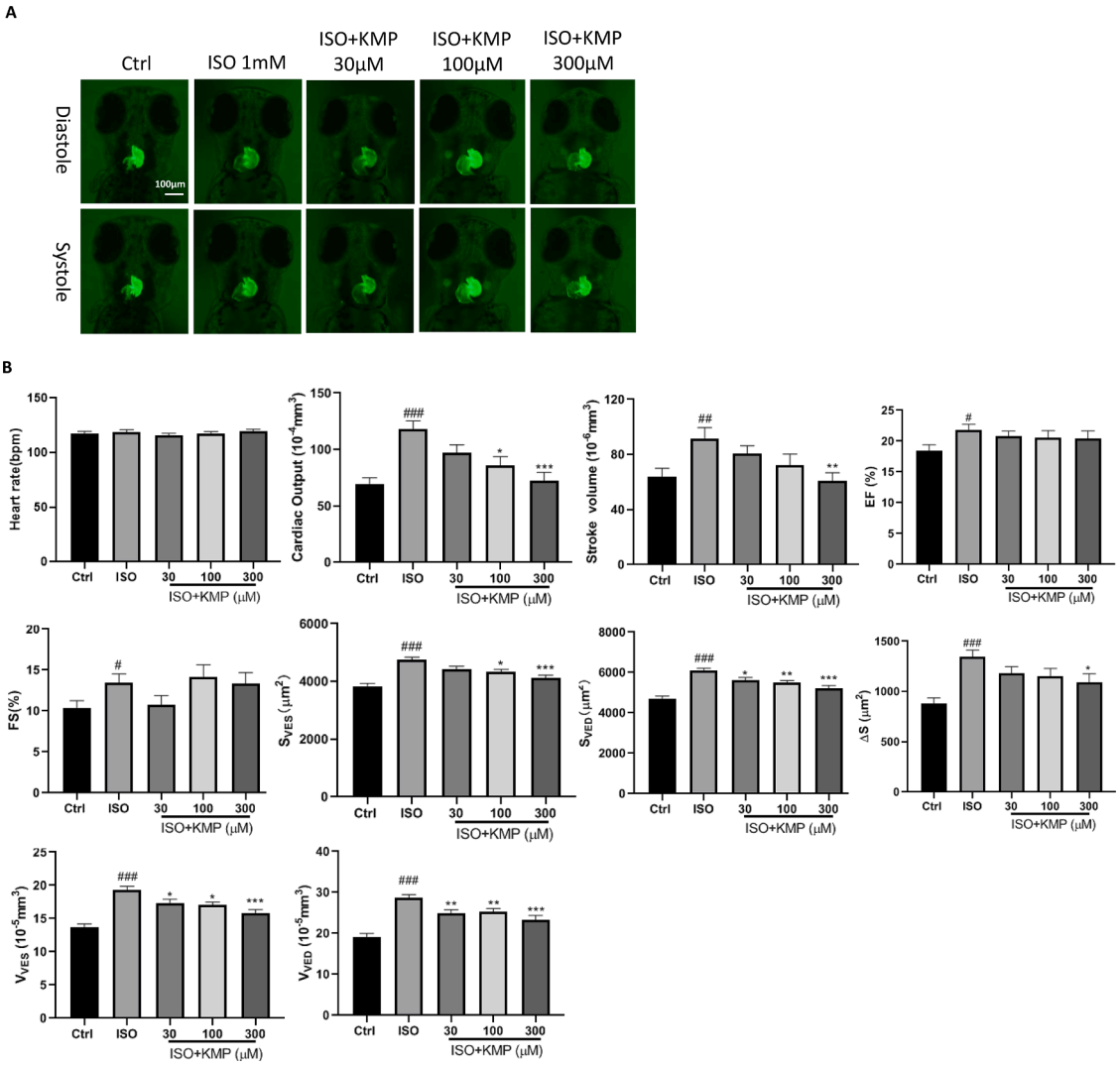

Fig. 5. The protective effect of kaempferol (KMP) on ISO-induced cardiac hypertrophy and dysfunction in zebrafish. (A) The pictures demonstrated the end-diastolic and systolic image of ventricle in various treatment groups. (B) Twenty-four hpf zebrafish Tg(*cmlc2*: GFP) embryos were treated with ISO (1 mM), with or without various concentrations (30, 100 and 300 μM) of KMP, for 48 h, then the cardiac morphology was observed by an inverted fluorescence microscope as well as the calculation of heart rate, cardiac output, stroke volume, EF, FS, S_{VED}, S_{VES}, ΔS, V_{VED} and V_{VES}. All the data were presented as mean ± SEM. $\#p < 0.05$, $\#\#p < 0.01$ and $\#\#\#p < 0.001$ *vs* control (Ctrl) group; $*p < 0.05$, $**p < 0.01$ and $***p < 0.001$ *vs* ISO-treated group. $n = 4$–6.

Propranolol (PRO), which is a beta-blocker and widely used for treatment of heart failure, served as the positive control. Consistently, ISO treatment significantly elevated the mRNA expression levels of cardiac injury markers including C-type natriuretic peptide (*cnp*), creatine kinase MB (*ckmb*) and cardiac troponin T 2 (*ctnt2*), while co-treatment with QXY (600 μg/ml) significantly reduced the expression of these genes (Fig. 1E). These results indicated that QXY extract effectively prevented ISO-induced cardiac hypertrophy, dysfunction and injury.

Identification and quantification of the main contents of QXY by UHPLC-MS

The QXY formula contains nine Chinese Materia Medica listed in Table 1. UHPLC-MS was applied to analyze the major constitutes in QXY extract. The total iron current and selected iron monitoring (SIM) were performed for quantification and identification (Fig. 2A and B). Eight compounds, including benzoylmesaconine (BMA), atractylenolide I (ATL I), icariin (ICA), quercitrin (QUE), psoralen (PRN), kaempferol (KMP), ferulic acid (FA) and protocatechuic acid (PCA) were identified in QXY extract (Fig. 2C and D). Their amounts were 124.44 ± 6.48 μg/g, 0.42 ± 0.06 μg/g, 1036.95 ± 69.44 μg/g, 78.14 ± 0.79 μg/g, 984.30 ± 6.14 μg/g, 3.18 ± 0.21 μg/g, 415.90 ± 21.74 μg/g and 39.86 ± 0.78 μg/g, respectively (Fig. 3A and Table 3). The top three ingredients of QXY extract were ICA, PRN and FA (Table 3). Toxicity analyses in zebrafish revealed that the maximum non-toxic concentrations of BMA, ATL I, ICA, QUE, PRN, KMP, FA and PCA were 300 μM, 10 μM, 300 μM, 300 μM, 30 μM, 100 μM, 300 μM and 300 μM, respectively (Fig. 3B). Thus, non-toxic concentrations of these compounds were used to test their protective activities against ISO-induced cardiac hypertrophy in zebrafish.

Identification of the main active ingredients of QXY protecting against ISO-caused cardiac hypertrophy and dysfunction in zebrafish

In vivo, the glycosides ICA and QUE were hydrolyzed to form aglycons icaritin (ICT) and quercitin (QCT) respectively (Bi et al., 2022; Dai et al., 2021). Next, the cardiac protective functions of all eight compounds plus ICT and QCT, were examined using ISO-treated zebrafish model (Figs. 4–6**, and S1-S7**). The results demonstrated that PRN and KMP significantly decreased the cardiac output, stroke volume, EF, S_{VED}, S_{VES}, ΔS, V_{VED} and V_{VES} on ISO-induced cardiac hypertrophy in zebrafish (Figs, 4 and 5). Interestingly, although ICA did not affect

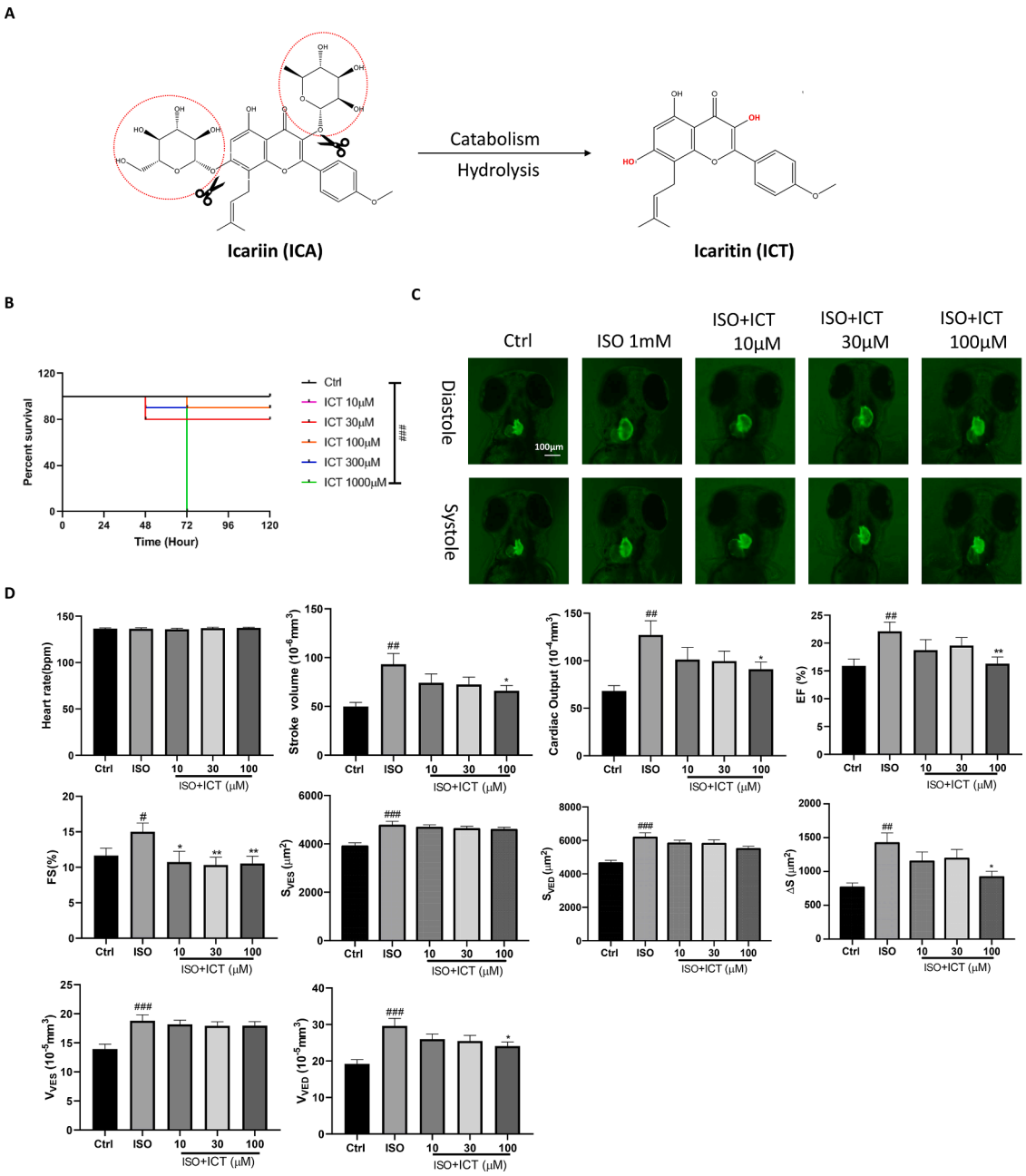

Fig. 6. The protective effect of icaritin (ICT) on ISO-induced cardiac hypertrophy and dysfunction in zebrafish. (A) The demonstration of ICA catalyzed to ICT by hydrolysis of the glucose groups. (B) The survival curve of 24 hpf zebrafish WT embryos treated with various concentrations (10, 30, 100, 300 and 1000 μM) of ICT for 5 days. (C) The pictures demonstrated the end-diastolic and systolic image of ventricle in various treatment groups. (D) Twenty-four hpf zebrafish Tg(*cmlc2*: GFP) embryos were treated with ISO (1 mM), with or without various concentrations (10, 30 and 100 μM) of ICT, for 48 h, then the cardiac morphology were observed by an inverted fluorescence microscope as well as the calculation of heart rate, cardiac output, stroke volume, EF, FS, S_{VED}, S_{VES}, ΔS, V_{VED} and V_{VES}. All the data were presented as mean ± SEM. $\#p < 0.05$, $\#\#p < 0.01$ and $\#\#\#p < 0.001$ *vs* control (Ctrl) group; $*p < 0.05$ and $**p < 0.01$ *vs* ISO-treated group. $n = 4$–6.

ISO-induced cardiac hypertrophy (**Figure S**1), its catabolite ICT significantly reduced ISO-induced elevation of cardiac output, stroke volume, EF, ΔS and V_{VES} in zebrafish with low toxicity (Fig. 6). Taken together, PRN, KMP and ICA might be the active constitutes of QXY extract preventing cardiac injury.

QXY inhibited calcium influx and mitochondrial dysfunction in H9c2 cardiomyocyte

To determine the potential pharmacological targets of QXY, we performed transcriptomic analysis by RNA-seq technology in zebrafish. Approximately 91.80 % sequences matched with annotated genes in the Genome assembly GRCz11 (Submitted GenBank assembly GCA_000002035.4) and 25,619 genes were detected in total. Eighty-nine differentially expressed genes (DEGs) were identified between the QXY-treated and control groups in which 43 genes were upregulated and 46 genes downregulated by QXY treatment. These DEGs were visualized by volcano plot and further analysis by GO enrichment (Fig. 7A). The results indicated that QXY might target the Ca^{2+}-related signaling and proteins. Thus, the effect of QXY on the intracellular Ca^{2+} influx was analyzed in H9c2 cardiomyocyte.

ISO specifically actives beta-andrenegic receptor and triggers Ca^{2+} influx through L-type calcium channel (Zhou et al., 2009). Consistently, we found that ISO triggered the calcium influx in H9c2 cells whereas

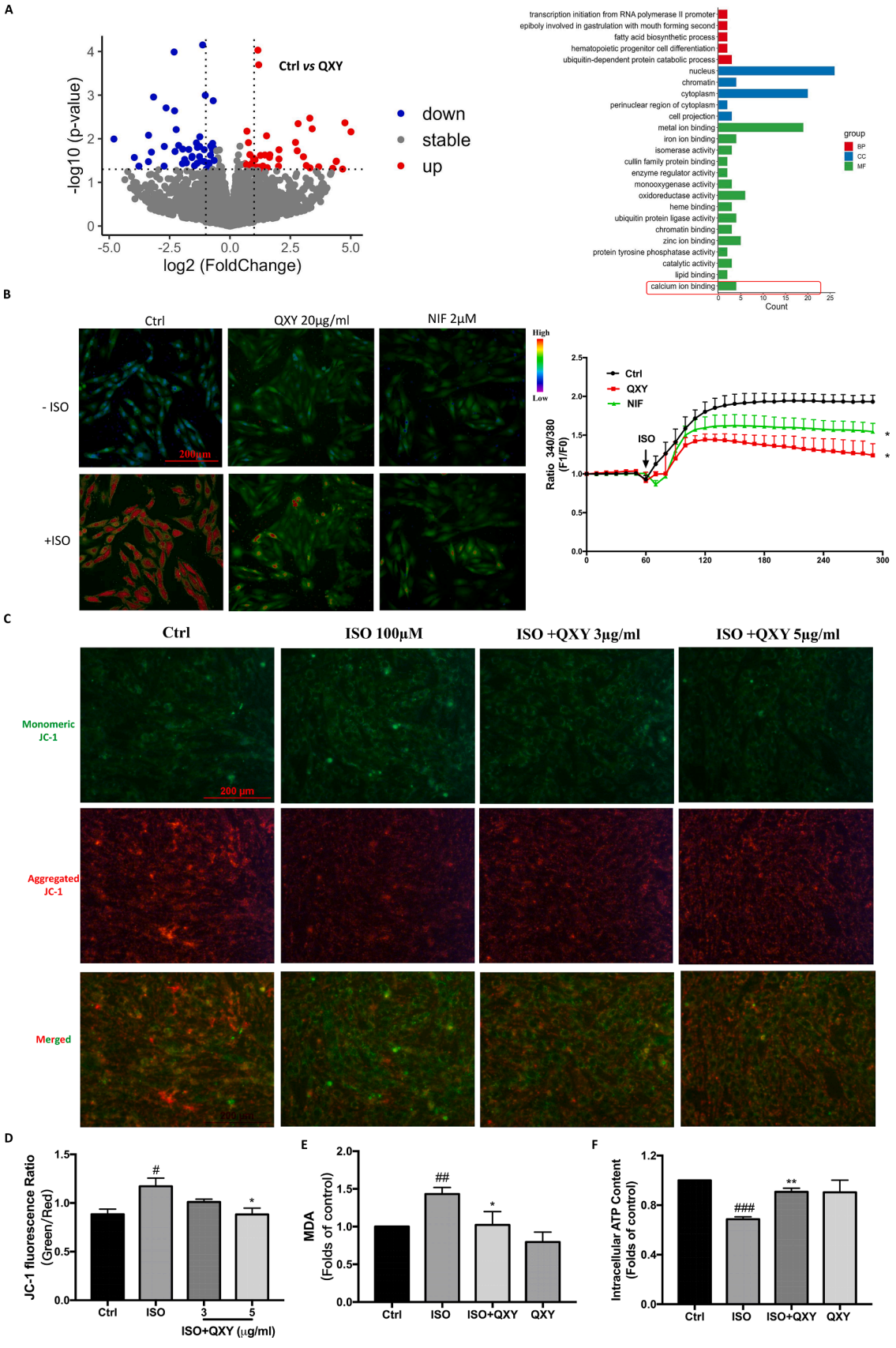

(caption on next page)

Fig. 7. The protective effect of QXY on ISO-induced calcium influx and mitochondrial dysfunction in H9c2 cells. (A) The transcriptome profile of the regulation of gene expression and its GO enrichment of differentially expressed genes (DEGs) between QXY-treated and control groups. Red rectangle presented that DEGs were enriched with the item of calcium binding. (B) The intracellular calcium imaging of H9c2 cells, which were pre-treated with QXY (20 μg/ml) or nifedipine (NIF, 2 μM) for 15 min, challenged with ISO (1 μM). The L-type calcium channel blocker NIF served as the positive control. The intracellular Ca^{2+} change was presented as the real-time fluorescence intensity (F1) to the fluorescence intensity before stimulation (F0), which indicated by the color change in the real-time imaging. (C-D) The H9c2 cells were treated with ISO (100 μM), with or without QXY (3 μg/ml, 5 μg/ml), for 24 h. The mitochondrial membrane potential were detected by JC-1 staining and calculated by the fluorescence intensity ratio of Green (monomeric JC-1) / Red (aggregated JC-1). (E-F) The H9c2 cells were treated with ISO (100 μM), with or without QXY (5 μg/ml), for 24 h. Then the cells were harvested and followed by intracellular MDA and ATP assays according to the manufactures. All the data were presented as mean ± SEM. $\#p < 0.05$, $\#\#p < 0.01$ and $\#\#\#p < 0.001$ *vs* control (Ctrl) group; $^{*}p < 0.05$ and $^{**}p < 0.01$ *vs* ISO-treated group. $n = 4–6$.

pre-treatment with QXY (5 μg/ml) significantly inhibited the ISO-induced intracellular Ca^{2+} elevation (Fig. 7B). The L-type calcium channel blocker nifedipine (NIF) was served as the positive control. Calcium influx and overload impact mitochondrial function and oxidative stress in cardiomyocyte (Dridi et al., 2023). ISO disrupted the mitochondrial membrane potential, which was prevented by co-treatment with QXY (Fig. 7C and D). QXY (5 μg/ml) significantly decreased intracellular MDA contents (Fig. 7E) and protected against the reduction of intracellular ATP in ISO-treated cardiomyocytes (Fig. 7F). These results suggested that QXY inhibited calcium influx and mitochondrial dysfunction.

QXY suppressed ISO-induced hypertrophy and cytoskeleton reorganization

Cardiac hypertrophy is characterized by cell hypertrophy and cytoskeleton reorganization in cardiomyocyte (Kooij et al., 2016). The results showed that ISO treatment significantly increased the cytoskeleton area and protein concentration in H9c2 cardiomyocytes, which were prevented by co-treatment with QXY (5 μg/ml) (Fig. 8A). The Smad family member 2 (SMAD2) and RhoA/Rho-kinase (ROCK) signaling pathways are involved in cellular process of cell hypertrophy and cytoskeleton reorganization (Amano et al., 2010; Duran et al., 2018). Co-treatment of QXY with ISO significantly increased the phosphorylation of SMAD2 when compared with ISO-treated group (Fig. 8B). The cardiac fibrosis markers, α-SMA and vimentin (Ding et al., 2020), were not significantly changed in all groups (Fig. 8B). Moreover, co-treatment of QXY with ISO increased the phosphorylation of myosin phosphatase subunit 1 (MYPT1) while decreased the phosphorylation of myosin light chain (MLC) (Fig. 8C). However, QXY did not affect the reduction of ROCK1 by ISO and the amount of RhoA (Fig. 8C). These results revealed that QXY significantly inhibited the cardiomyocyte hypertrophy and cytoskeleton reorganization at least partly by regulation of SMAD2 and ROCK signaling pathways.

Discussion

Heart failure is a severe outcome of cardiovascular disease and characterized by cardiac hypertrophy. Traditional Chinese medicine, such as QXY formula, provides an alternative medication for heart failure based on its thousands of years' clinical application. In the this study, we explored the underlying mechanisms of QXY formula as well as its active ingredients.

Zebrafish has emerged as an attractive model for the study of cardiovascular disease due to its advantages including genetic similarity with human, lower cost, transparent embryos and short experimental period (Kossack et al., 2017). In this study, we employed the transgenic zebrafish embryos with specific expression of GFP in cardiomyocyte. The β-adrenergic receptor activator ISO-induced cardiac hypertrophy model was applied (Kossack et al., 2017) (Fig. 1**A**). We found that QXY has low toxicity on zebrafish embryo within the concentration range ≤ 600 μg/ml (Fig. 1B), and significantly blocked ISO -induced cardiac dysfunction and injury in zebrafish (Fig. 1**C, D and E**). QXY exerts cardiac protective activity in a concentration-dependent manner.

The well-known feature of traditional Chinese medicine is the complex ingredients. Thus, we analyzed the chemical profile of QXY using UHPLC-MS (Fig. 2). The main constitutes were BMA, ATL I, ICA, QUE, PRN, KMP, FA and PCA (Fig. 2 and Table 3), in which ICA, PRN and FA represent the top three ingredients. The quantification of the ingredient of QXY is beneficial as a quality control for further drug development. In order to clarify the active constitutes of QXY, we evaluated the toxicity of these eight constitutes in zebrafish embryos (Fig. 3B) and screened their anti-cardiac hypertrophy effects using ISO-induced cardiac hypertrophy zebrafish model. ICT and QCT, which were the hydrolysis metabolite of ICA and QUE respectively, were also included (Figs. 4–6 and **S1–S7**). We found that PRN, KMP and ICT, significantly protected against ISO-induced cardiac hypertrophy and dysfunction (Figs. 4–6). PRN is one of the active constitutes of Chinese Materia Medica PSORALEAE FRUCTUS, which is the dry matured fruit of *Psoralea corylifolia* L. (Committee, 2020), with potent hepatotoxicity (Guo et al., 2021). We reported its cardiac protective effect against ISO-induced cardiac hypertrophy for the first time. Further study is needed for the treatment window of PRN for cardiac hypertrophy as well as its molecular structure-toxicity relationship. KMP belongs to flavonoid and widely exists in multiple Chinese Materia Medica, including PAEONIAE RADIX ALBA, with various pharmacological activities such as anti-cancer (Imran et al., 2019), anti-diabetes (Yang et al., 2022), anti-microbial (Periferakis et al., 2022) and anti-neurodegenerative disease (Dong et al., 2023). The anti-cardiac hypertrophy activity of KMP might result from its anti-oxidative (Chagas et al., 2022) and anti-inflammation (Alam et al., 2020) effects according to previous studies (Dabeek and Marra, 2019). ICT is the hydrolysis product of ICA, which is the main active component of Chinese Materia Medica EPIMEDII FOLIUM (Committee, 2020). Interestingly, ICT presented significant anti-cardiac hypertrophy effect while ICA not presented this activity (**Fig. S1**) although they are structural similarity. The metabolic process of compound is complex in zebrafish although the metabolic pathway is similar with mammalian (Li et al., 2011). Taken together, these results suggest that PRN, KMP and ICA are the main active ingredients of QXY preventing cardiac hypertrophy, which can be used for the bioactive markers of QXY in its further drug development.

Pan-omics analysis including transcriptome, metabolome and proteome are useful tools for mechanistic study of traditional Chinese medicine treating disease (Zhou et al., 2019a; 2020b; 2020c). Regarding the underlying mechanisms of QXY protecting against cardiac hypertrophy, we profiled the transcriptome of QXY treatment in zebrafish and found that the DEGs were enriched in item of calcium binding (Fig. 7**A**). Consistently, QXY dramatically blocked the calcium influx that stimulated by ISO, and the calcium influx blockage effect of QXY was strong than L-type calcium channel inhibitor NIF (Fig. 7**B**). The intracellular calcium overload, which is caused by calcium influx, attributes to cardiomyocyte injury by disruption of mitochondria function, leading to the intracellular ROS accumulation, lipid peroxidation and ATP reduction (Fu et al., 2023; Li et al., 2024). In this study, we also found that ISO impaired the mitochondrial membrane potential, lipid peroxidation (MDA) and ATP production, while these pathological changes were almost abolished by QXY (Fig. 7**C-F**). These results suggest that the blockage of calcium influx and preventing calcium overload might play vital roles in QXY protecting against cardiac hypertrophy.

Moreover, the increased intracellular calcium affects cardiomyocyte contractile machinery and cytoskeleton reorganization (Sequeira et al.,

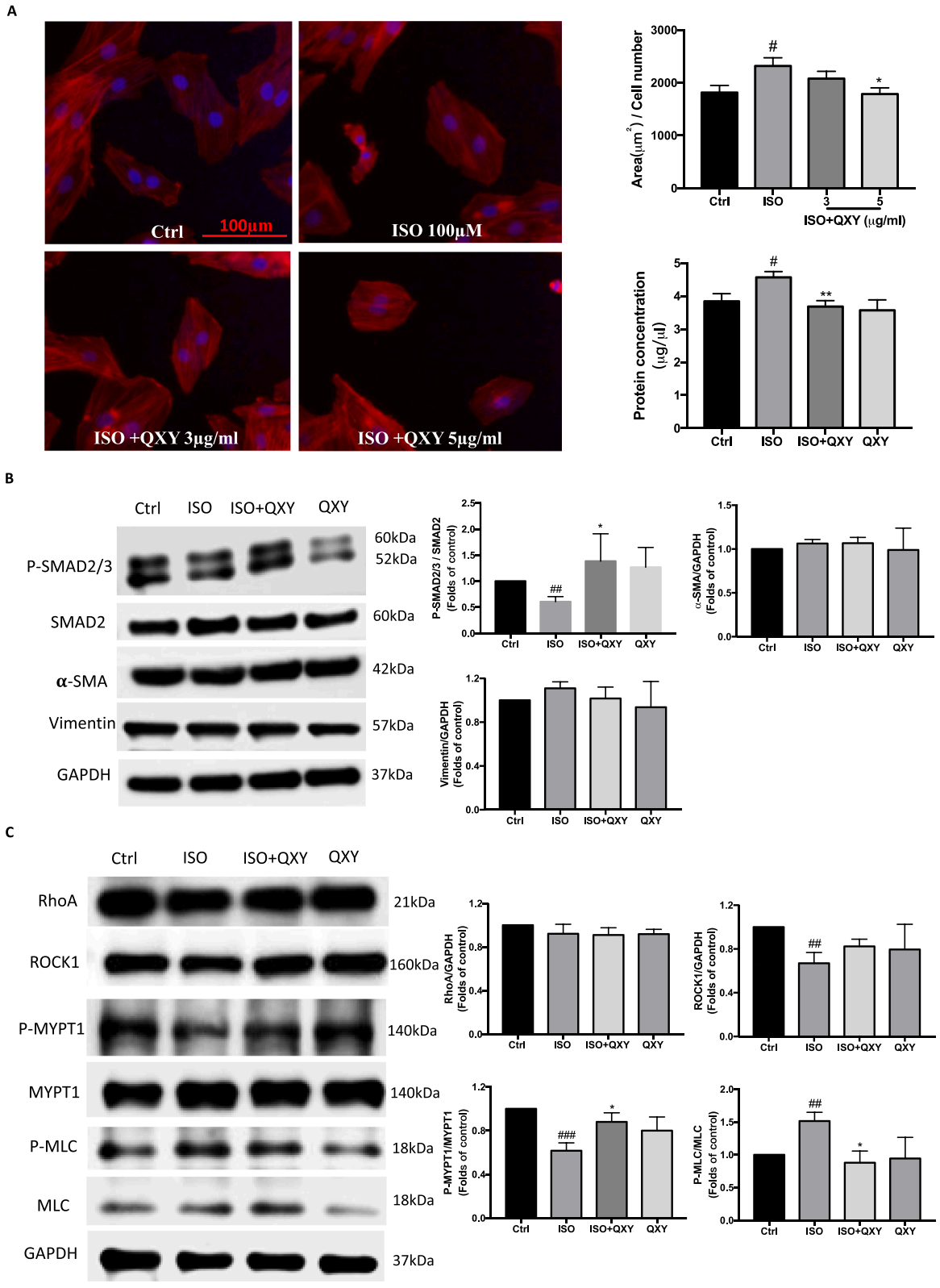

Fig. 8. The protective effect and mechanism of QXY on ISO-induced cytoskeleton reorganization and hypertrophy in H9c2 cells. (A) The H9c2 cells were treated with ISO (100 μM), with or without QXY (3 μg/ml, 5 μg/ml), for 24 h. The intracellular cytoskeleton and nuclei were stained with Actin-Tracker Red-Rhodamine and DAPI, respectively. The protein concentration of cells was measured by BCA analysis. (B-C) The H9c2 cells were treated with ISO (100 μM), with or without QXY (5 μg/ml), for 24 h. The protein expression levels of phosphor-SMAD2/3, SMAD2, α-SMA, Vimentin, RhoA, ROCK1, phosphor-MYPT1, MYPT1, phosphor-MLC, and MLC were detected by western blotting. GAPDH served as the internal control. All the data were presented as mean ± SEM. $\#p < 0.05$, $\#\#p < 0.01$ and $\#\#\#p < 0.001$ *vs* control (Ctrl) group; $*p < 0.05$ and $**p < 0.01$ *vs* ISO-treated group. $n = 4–6$.

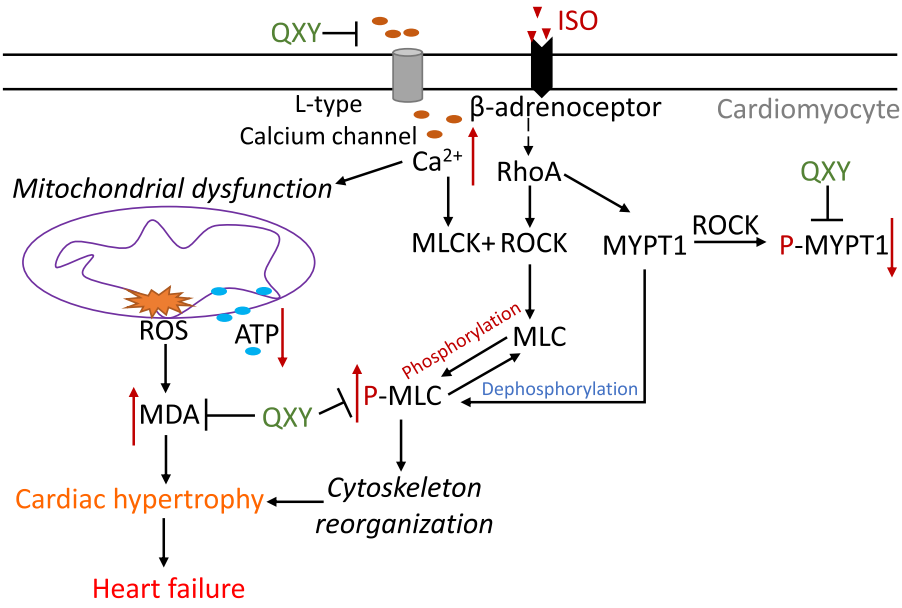

Fig. 9. Schematic overview of the underlying mechanisms of QXY protecting against ISO-induced cardiac hypertrophy and heart failure.

2014). QXY inhibited the ISO-induced cytoskeleton reorganization and hypertrophy in cardiomyocyte (Fig. 8**A**). Previous studies indicated that ISO led to the cardiac fibrosis and hypertrophy via the activation of SMAD2 in rat (Meshram et al., 2022). But, we found that the ISO inhibited the activation of SMAD2 and not affected the fibrosis markers including α-SMA and vimentin (Fig. 8**B**). The reason might be the acute treatment of high concentration of ISO that mainly affected the cell viability in this study since the SMAD2 signaling is also important for cell growth (Thien et al., 2015; Zhang et al., 2021). Although QXY increased the phosphorylation of SMAD2, the fibrosis markers α-SMA and vimentin were also not significant changed (Fig. 8**B**). In addition, ISO increased the phosphorylation of MLC, which are the indicator of ROCK signaling activation and cytoskeleton reorganization (Huang et al., 2018; Zhou et al., 2018), and QXY dramatically inhibited MLC phosphorylation (Fig. 8**C**). QXY also suppressed the ISO-induced the phosphorylation of MYPT1 regardless of RhoA and ROCK1 (Fig. 8**C**). These results revealed that QXY was likely to inhibit ISO-induced ROCK activation signaling. The inhibition of ROCK signaling has been proved with great therapeutic potential in cardiovascular disease including cardiac hypertrophy and heart failure (Hartmann et al., 2015; Surma et al., 2011). Taken together, QXY might inhibit the calcium overload and its associated mitochondrial dysfunction as well as ROCK-related cytoskeleton reorganization in the treatment of cardiac hypertrophy (Fig. 9). However, these regulations are just partially though attenuation of RhoA/ROCK/MYPT1/MLC signaling cascade. In the current study, the pharmacokinetic study has not been included, which is vital for the elucidating the active ingredients of QXY as well as the underlying mechanism. If the pharmacokinetic and pharmacodynamic study of QXY, such as ADME (absorbance, distribution, metabolism and elimination), has been completed in mice or rat, the drug-containing serum can be employed for the mechanistic study in cardiomyocyte. Although the anti-cardiac hypertrophy effect of QXY and its underlying mechanism has been partially elucidated in zebrafish and cardiomyocyte, the verification in mice or rat should be conducted in the future.

Conclusion

PRN, KMP and ICT are the main active ingredients of QXY protecting against cardiac hypertrophy. The underlying mechanism of QXY preventing cardiac hypertrophy is involved in the blockage of calcium influx, and subsequent inhibition of mitochondrial dysfunction and cytoskeleton reorganization. Our findings provide evidence for the clinical usage of QXY for the treatment of heart failure and are beneficial for the quality control and further drug development of QXY.

CRediT authorship contribution statement

Zhong-Yan Zhou: Writing – review & editing, Writing – original draft, Resources, Project administration, Methodology, Investigation. **Jie Ma:** Writing – review & editing, Resources, Project administration, Funding acquisition. **Wai-Rong Zhao:** Writing – original draft, Visualization, Validation, Investigation, Formal analysis, Data curation. **Wen-Ting Shi:** Methodology, Investigation, Data curation. **Jing Zhang:** Validation, Investigation. **Yan-Yan Hu:** Methodology, Investigation. **Mei-Yan Yue:** Visualization, Conceptualization. **Wen-Long Zhou:** Validation. **Hua Yan:** Project administration, Methodology. **Jing-Yi Tang:** Supervision, Resources, Project administration, Funding acquisition. **Yu Wang:** Writing – review & editing, Writing – original draft, Supervision, Resources, Project administration, Methodology, Formal analysis.

Declaration of competing interest

The authors have declared no conflict of interest.

Acknowledgments

This study was supported by Shanghai Municipal Science and Technology Commission (21ZR1463200), Shanghai University of Traditional Chinese Medicine (2021LK049), Shanghai Municipal Health Commission (GWIV-28, inheritance and innovation of Prof. Yan Shiyun's academic experience), Shanghai Human Resources and Social Security Bureau (Pujiang Project, 2023PJD094) and Organizational Key Research and Development Program of Shanghai University of Traditional Chinese Medicine (2023YZZ02). Thanks for Prof. Tao Yang from Shuguang Hospital, Shanghai University of Traditional Chinese Medicine for the support of chemical analysis of constitutes in QXY formula by UHPLC-MS technology.

Supplementary materials

Supplementary material associated with this article can be found, in

the online version, at doi:10.1016/j.phymed.2024.155717.

References

Alam, W., Khan, H., Shah, M.A., Cauli, O., Saso, L., 2020. Kaempferol as a dietary anti-inflammatory agent: current therapeutic standing. Molecules 25.

Amano, M., Nakayama, M., Kaibuchi, K., 2010. Rho-kinase/ROCK: a key regulator of the cytoskeleton and cell polarity. Cytoskeleton 67, 545–554 (Hoboken).

Bauersachs, J., 2021. Heart failure drug treatment: the fantastic four. Eur. Heart. J. 42, 681–683.

Bi, Z., Zhang, W., Yan, X., 2022. Anti-inflammatory and immunoregulatory effects of icariin and icaritin. Biomed. Pharmacother. 151, 113180.

Chagas, M., Behrens, M.D., Moragas-Tellis, C.J., Penedo, G.X.M., Silva, A.R., Gonçalves-de-Albuquerque, C.F., 2022. Flavonols and flavones as potential anti-inflammatory, antioxidant, and antibacterial compounds. Oxid. Med. Cell Longev. 2022, 9966750.

Cheng, Y., Wu, X., Nie, X., Wu, Y., Zhang, C., Lee, S.M., Lv, K., Leung, G.P., Fu, C., Zhang, J., Li, J., 2022. Natural compound glycyrrhetinic acid protects against doxorubicin-induced cardiotoxicity by activating the Nrf2/HO-1 signaling pathway. Phytomedicine 106, 154407.

Committee, C.P., 2020. The Chinese Pharmacopoeia 2020 edition. China Medical Science and Technology Press, Beijing, China. Traditional Chinese Medicines Including materials, Cut Crude drugs, Vegetable Olils and extracts, Formulation Preparation and Single Flavour Preparaton.

Dabeek, W.M., Marra, M.V., 2019. Dietary quercetin and kaempferol: bioavailability and potential cardiovascular-related bioactivity in humans. Nutrients 11.

Dai, T., Wang, M., Wang, P., Dai, L., Dai, R., Meng, Q., 2021. Inhibition effects of eight anti-coronavirus drugs on glycosides metabolism and glycosidases in human gut microflora. Pharmazie 76, 195–201.

Ding, Y., Wang, Y., Zhang, W., Jia, Q., Wang, X., Li, Y., Lv, S., Zhang, J., 2020. Roles of biomarkers in myocardial fibrosis. Aging Dis. 11, 1157–1174.

Dong, X., Zhou, S., Nao, J., 2023. Kaempferol as a therapeutic agent in Alzheimer's disease: evidence from preclinical studies. Ageing Res. Rev. 87, 101910.

Dridi, H., Santulli, G., Bahlouli, L., Miotto, M.C., Weninger, G., Marks, A.R., 2023. Mitochondrial calcium overload plays a causal role in oxidative stress in the failing heart. Biomolecules 13.

Duran, J., Troncoso, M.F., Lagos, D., Ramos, S., Marin, G., Estrada, M., 2018. GDF11 modulates Ca(2+)-dependent smad2/3 signaling to prevent cardiomyocyte hypertrophy. Int. J. Mol. Sci. 19.

Fu, D., Luo, J., Wu, Y., Zhang, L., Li, L., Chen, H., Wen, T., Fu, Y., Xiong, W., 2023. Angiotensin II-induced calcium overload affects mitochondrial functions in cardiac hypertrophy by targeting the USP2/MFN2 axis. Mol. Cell Endocrinol. 571, 111938.

Guo, Z., Li, P., Wang, C., Kang, Q., Tu, C., Jiang, B., Zhang, J., Wang, W., Wang, T., 2021. Five constituents contributed to the psoraleae fructus-induced hepatotoxicity via mitochondrial dysfunction and apoptosis. Front. Pharmacol. 12.

Hartmann, S., Ridley, A.J., Lutz, S., 2015. The function of Rho-associated kinases ROCK1 and ROCK2 in the pathogenesis of cardiovascular disease. Front. Pharmacol. 6, 276.

Hu Jinping, C.L., Youlong, P., Shengming, L., Shiyun, Y., 2023. Study on the effect and mechanism of Qiangxinyin on echocardiography and myocardial cell apoptosis in chronic heart failure model rats. Shizhen Chin. Med. 34, 296–299.

Huang, B., Zhou, Z.Y., Li, S., Huang, X.H., Tang, J.Y., Hoi, M.P.M., Lee, S.M.Y., 2018. Tanshinone I prevents atorvastatin-induced cerebral hemorrhage in zebrafish and stabilizes endothelial cell-cell adhesion by inhibiting VE-cadherin internalization and actin-myosin contractility. Pharmacol. Res. 128, 389–398.

Imran, M., Salehi, B., Sharifi-Rad, J., Aslam Gondal, T., Saeed, F., Imran, A., Shahbaz, M., Tsouh Fokou, P.V., Umair Arshad, M., Khan, H., Guerreiro, S.G., Martins, N., Estevinho, L.M., 2019. Kaempferol: a key emphasis to its anticancer potential. Molecules 24.

Jia, Q., Wang, L., Zhang, X., Ding, Y., Li, H., Yang, Y., Zhang, A., Li, Y., Lv, S., Zhang, J., 2020. Prevention and treatment of chronic heart failure through traditional Chinese medicine: role of the gut microbiota. Pharmacol. Res. 151, 104552.

Kooij, V., Viswanathan, M.C., Lee, D.I., Rainer, P.P., Schmidt, W., Kronert, W.A., Harding, S.E., Kass, D.A., Bernstein, S.I., Van Eyk, J.E., Cammarato, A., 2016. Profilin modulates sarcomeric organization and mediates cardiomyocyte hypertrophy. Cardiovasc. Res. 110, 238–248.

Kossack, M., Hein, S., Juergensen, L., Siragusa, M., Benz, A., Katus, H.A., Most, P., Hassel, D., 2017. Induction of cardiac dysfunction in developing and adult zebrafish by chronic isoproterenol stimulation. J. Mol. Cell Cardiol. 108, 95–105.

Li, Z., Hu, O., Xu, S., Lin, C., Yu, W., Ma, D., Lu, J., Liu, P., 2024. The SIRT3-ATAD3A axis regulates MAM dynamics and mitochondrial calcium homeostasis in cardiac hypertrophy. Int. J. Biol. Sci. 20, 831–847.

Li, Z.H., Alex, D., Siu, S.O., Chu, I.K., Renn, J., Winkler, C., Lou, S., Tsui, S.K., Zhao, H.Y., Yan, W.R., Mahady, G.B., Li, G.H., Kwan, Y.W., Wang, Y.T., Lee, S.M., 2011. Combined *in vivo* imaging and omics approaches reveal metabolism of icaritin and its glycosides in zebrafish larvae. Mol. Biosyst. 7, 2128–2138.

Ling, D., Chen, H., Chan, G., Lee, S.M., 2022. Quantitative measurements of zebrafish heartrate and heart rate variability: a survey between 1990 and 2020. Comput. Biol. Med. 142, 105045.

McLellan, M.A., Skelly, D.A., Dona, M.S.I., Squiers, G.T., Farrugia, G.E., Gaynor, T.L., Cohen, C.D., Pandey, R., Diep, H., Vinh, A., Rosenthal, N.A., Pinto, A.R., 2020. High-resolution transcriptomic profiling of the heart during chronic stress reveals cellular drivers of cardiac fibrosis and hypertrophy. Circulation 142, 1448–1463.

Meshram, S., Verma, V.K., Mutneja, E., Sahu, A.K., Malik, S., Mishra, P., Bhatia, J., Arya, D.S., 2022. Evidence-based mechanistic role of chrysin towards protection of cardiac hypertrophy and fibrosis in rats. Br. J. Nutr. 1–14.

Periferakis, A., Periferakis, K., Badarau, I.A., Petran, E.M., Popa, D.C., Caruntu, A., Costache, R.S., Scheau, C., Caruntu, C., Costache, D.O., 2022. Kaempferol: antimicrobial properties, sources, clinical, and traditional applications. Int. J. Mol. Sci. 23.

Rosano, G.M.C., Allen, L.A., Abdin, A., Lindenfeld, J., O'Meara, E., Lam, C.S.P., Lancellotti, P., Savarese, G., Gottlieb, S.S., Teerlink, J., Wintrich, J., Böhm, M., 2021. Drug Layering in Heart Failure: phenotype-Guided Initiation. JACC Heart. Fail. 9, 775–783.

Savarese, G., Becher, P.M., Lund, L.H., Seferovic, P., Rosano, G.M.C., Coats, A.J.S., 2023. Global burden of heart failure: a comprehensive and updated review of epidemiology. Cardiovasc. Res. 118, 3272–3287.

Sequeira, V., Nijenkamp, L.L., Regan, J.A., van der Velden, J., 2014. The physiological role of cardiac cytoskeleton and its alterations in heart failure. Biochim. Biophys. Acta 1838, 700–722.

Surma, M., Wei, L., Shi, J., 2011. Rho kinase as a therapeutic target in cardiovascular disease. Future Cardiol. 7, 657–671.

Sutton, N.R., Malhotra, R., St Hilaire, C., Aikawa, E., Blumenthal, R.S., Gackenbach, G., Goyal, P., Johnson, A., Nigwekar, S.U., Shanahan, C.M., Towler, D.A., Wolford, B.N., Chen, Y., 2023. Molecular mechanisms of vascular health: insights from vascular aging and calcification. Arterioscler. Thromb. Vasc. Biol. 43, 15–29.

Thien, A., Prentzell, M.T., Holzwarth, B., Kläsener, K., Kuper, I., Boehlke, C., Sonntag, A. G., Ruf, S., Maerz, L., Nitschke, R., Grellscheid, S.N., Reth, M., Walz, G., Baumeister, R., Neumann-Haefelin, E., Thedieck, K., 2015. TSC1 activates TGF-β-Smad2/3 signaling in growth arrest and epithelial-to-mesenchymal transition. Dev. Cell 32, 617–630.

Wang, L., Zhang, X., Chan, J.Y., Shan, L., Cui, G., Cui, Q., Wang, Y., Li, J., Chen, H., Zhang, Q., Yu, P., Han, Y., Wang, Y., Lee, S.M., 2016. A Novel danshensu derivative prevents cardiac dysfunction and improves the chemotherapeutic efficacy of doxorubicin in breast cancer cells. J. Cell Biochem. 117, 94–105.

Wang, Y., Wang, Q., Li, C., Lu, L., Zhang, Q., Zhu, R., Wang, W., 2017. A review of Chinese herbal medicine for the treatment of chronic heart failure. Curr. Pharm. Des. 23, 5115–5124.

Yan Hua, G.J., 2011. Effect of Qiangxin Yin on apoptotic factors in cardiomyopathy rat model. Chin. Med. Guide 9, 71–72.

Yan Shiyun, S.Y., Deyu, Fu, Minzhi, R., 2004. Clinical observation on 38 cases of chronic cardiac failure treated with Qiangxinyin. Jiangxi Tradit. Chin. Med. 4, 8–9.

Yang, Y., Chen, Z., Zhao, X., Xie, H., Du, L., Gao, H., Xie, C., 2022. Mechanisms of Kaempferol in the treatment of diabetes: a comprehensive and latest review. Front. Endocrinol. 13, 990299 (Lausanne).

Zhang, J., Zhao, W.R., Shi, W.T., Tan, J.J., Zhang, K.Y., Tang, J.Y., Chen, X.L., Zhou, Z.Y., 2022. Tribulus terrestris L. extract ameliorates atherosclerosis by inhibition of vascular smooth muscle cell proliferation in ApoE(-/-) mice and A7r5 cells via suppression of Akt/MEK/ERK signaling. J. Ethnopharmacol. 297, 115547.

Zhang, L., Zhu, Z., Yan, H., Wang, W., Wu, Z., Zhang, F., Zhang, Q., Shi, G., Du, J., Cai, H., Zhang, X., Hsu, D., Gao, P., Piao, H.L., Chen, G., Bu, P., 2021. Creatine promotes cancer metastasis through activation of Smad2/3. Cell Metab. 33, 1111-1123 e1114.

Zhao, W.R., Shi, W.T., Zhang, J., Zhang, K.Y., Qing, Y., Tang, J.Y., Chen, X.L., Zhou, Z.Y., 2021. *Tribulus terrestris*L. Extract Protects against Lipopolysaccharide-Induced Inflammation in RAW 264.7 Macrophage and Zebrafish via Inhibition of Akt/MAPKs and NF-κB/iNOS-NO signaling pathways. Evid. Based Complement. Altern. Medicine 2021, 6628561.

Zhou, P., Zhao, Y.T., Guo, Y.B., Xu, S.M., Bai, S.H., Lakatta, E.G., Cheng, H., Hao, X.M., Wang, S.Q., 2009. Beta-adrenergic signaling accelerates and synchronizes cardiac ryanodine receptor response to a single L-type Ca2+ channel. Proc. Natl. Acad. Sci. U. S. A. 106, 18028–18033.

Zhou, Z.Y., Zhao, W.R., Xiao, Y., Zhang, J., Tang, J.Y., Lee, S.M.Y., 2020a. Mechanism study of the protective effects of sodium tanshinone IIA sulfonate against atorvastatin-induced cerebral hemorrhage in zebrafish: transcriptome analysis. Front. Pharmacol. 11.

Zhou, Z.Y., Huang, B., Li, S., Huang, X.H., Tang, J.Y., Kwan, Y.W., Hoi, P.M., Lee, S.M., 2018. Sodium tanshinone IIA sulfonate promotes endothelial integrity via regulating VE-cadherin dynamics and RhoA/ROCK-mediated cellular contractility and prevents atorvastatin-induced intracerebral hemorrhage in zebrafish. Toxicol. Appl. Pharmacol. 350, 32–42.

Zhou, Z.Y., Shi, W.T., Zhang, J., Zhao, W.R., Xiao, Y., Zhang, K.Y., Ma, J., Tang, J.Y., Wang, Y., 2023. Sodium tanshinone IIA sulfonate protects against hyperhomocysteine-induced vascular endothelial injury via activation of NNMT/SIRT1-mediated NRF2/HO-1 and AKT/MAPKs signaling in human umbilical vascular endothelial cells. Biomed. Pharmacother. 158, 114137.

Zhou, Z.Y., Xiao, Y., Zhao, W.R., Zhang, J., Shi, W.T., Ma, Z.L., Ye, Q., Chen, X.L., Tang, N., Tang, J.Y., 2019a. Pro-angiogenesis effect and transcriptome profile of Shuxinyin formula in zebrafish. Phytomedicine 65, 153083.

Zhou, Z.Y., Zhao, W.R., Shi, W.T., Xiao, Y., Ma, Z.L., Xue, J.G., Zhang, L.Q., Ye, Q., Chen, X.L., Tang, J.Y., 2019b. Endothelial-dependent and independent vascular relaxation effect of tetrahydropalmatine on rat aorta. Front. Pharmacol. 10, 336.

Zhou, Z.Y., Zhao, W.R., Xiao, Y., Zhang, J., Tang, J.Y., Lee, S.M., 2020b. Mechanism study of the protective effects of sodium tanshinone IIA sulfonate against atorvastatin-induced cerebral hemorrhage in zebrafish: transcriptome analysis. Front. Pharmacol. 11, 551745.

Zhou, Z.Y., Zhao, W.R., Xiao, Y., Zhou, X.M., Huang, C., Shi, W.T., Zhang, J., Ye, Q., Chen, X.L., Tang, J.Y., 2020c. Antiangiogenesis effect of timosaponin AIII on HUVECs *in vitro* and zebrafish embryos *in vivo*. Acta Pharmacol. Sin. 41, 260–269.